Shap. Mem. Superelasticity (2018) 4:272–284
https://doi.org/10.1007/s40830-018-0178-8

SPECIAL ISSUE: A TRIBUTE TO PROF. JAN VAN HUMBEECK – A LIFETIME OF CONTRIBUTIONS TO UNDERSTANDING MARTENSITE, INVITED PAPER

Remarks on the Particular Behavior in Martensitic Phase Transition in Cu-Based and Ni–Ti Shape Memory Alloys

Vicenç Torra[1,2] · Ferran Martorell[2] · Francisco C. Lovey[3] · Marcos Sade[3]

Published online: 29 May 2018

Abstract Many macroscopic behaviors of the martensitic transformations are difficult to explain in the frame of the classical first-order phase transformations, without including the role of point and crystallographic defects (dislocations, stacking faults, interfaces, precipitates). A few major examples are outlined in the present study. First, the elementary reason for thermoelasticity and pseudoelasticity in single crystals of Cu–Zn–Al (β-18R transformation) arises from the interaction of a growing martensite plate with the existing dislocations in the material. Secondly, in Cu–Al–Ni, the twinned hexagonal (γ′) martensite produces dislocations inhibiting this transformation and favoring the appearance of 18R in subsequent transformation cycles. Thirdly, single crystals of Cu–Al–Be visualize, via enhanced stress, a transformation primarily to 18R, a structural distortion of the 18R structure, and an additional transformation to another martensitic phase (i.e., 6R) with an increased strain. A dynamic behavior in Ni–Ti is also analyzed, where defects alter the pseudoelastic behavior after cycling.

Keywords Shape memory · Martensitic transformation · NiTi · CuAlBe · CuZnAl · CuAlNi · Mechanical behavior

✉ Vicenç Torra
vtorra_1@yahoo.com

[1] Department of Applied Physics, Polytechnical University of Catalonia, Barcelona, Spain

[2] Private Research Group, Villarroel 162, 08036 Barcelona, Spain

[3] Department of Materials Science, Centro Atomico de Bariloche, Instituto Balseiro and CONICET, San Carlos de Bariloche, Argentina

Introduction

The interest in shape memory alloys (SMA) has been increasing over the last four decades because of their potential use in medical and other industrial applications. This interest has recently been enhanced by the inclusion of standard courses on smart materials in the core engineering curriculum at many universities all over the world. The main property of SMA was associated to one martensitic transformation (MT), i.e., one structural change between solid phases. Martensitic transformations play a significant role in the field of solid–solid phase transitions, which are present in a large amount of materials. These transitions are characterized by singularities in one of the thermodynamic potentials, such as free energy, and hence by discontinuities in their derivatives. The pioneer work of P. Ehrenfest published in 1933 [1] classified phase transitions according to whether the first, second, etc. derivatives of the free energy showed a discontinuity and called them, respectively, first-order, second-order, etc. transitions. In the case of a first-order phase transition, the first derivative of the relevant thermodynamic potential is discontinuous.

Currently, it is noted that not only discontinuities but also divergences at the phase transition point are important. All higher-order phase transitions are grouped together as *critical* or *continuous* phase transitions. The term "continuous" phase transition was introduced by Landau in their classic paper on the theory of phase transitions [2]. The martensitic transformation is a phase transformation between solid metastable structures: parent and martensite in high and low temperature, respectively. It is considered a first-order phase transition and, in particular, in copper-based alloys the transformation is thermoelastic. That is, the transformation progresses following the undercooling below the equilibrium temperature, while elastic energy is

stored in the material. In this way, an intrinsic difference with the equilibrium conditions is established. In addition, a hysteresis is observed because of irreversible processes taking place during the transformation–retransformation path. These phenomena, which depend on the complexity of the problem and the related metastable phases, are time dependent. Reduction in complexity is thus necessary if intrinsic phenomena are to be separated and quantified.

In a single crystal, when the MT is thermally induced, the complexity is related to the coexistence of many martensite plates and residual parts of the parent structure, as it has been reported since a long time ago [3, 4]. This complexity impedes the separation of the intrinsic transformation phenomena from those that are produced by the mutual interaction between the plates. In fact, any increase of martensite phase amount introduces an increase of the interaction among martensite plates requiring a progressive cooling [5, 6]. An intrinsic thermoelasticity has been found in the single-interface transformation in Cu–Zn–Al single crystals. The phenomenon was ascribed to the interaction of growing martensite with the pre-existing dislocations. Dislocations show a paradoxical behavior in the MT. Classically, the dislocations were considered as a perturbation component, but in samples without dislocations, in very special circumstances, a break-down of the shape memory effect arises as will be commented below.

In this paper, a short review is presented, focusing on peculiar properties of the transformation behavior in shape memory alloys that escape from the classical expected behavior in first-order phase transition. A few examples will be considered in Cu-based alloys and also in the Ni–Ti system. In the frame of Cu-based alloys, three examples have been specifically chosen: (a) the single-interface transformation in Cu–Zn–Al single crystals induced by temperature changes, (b) the appearance of two martensite phases in Cu–Al–Ni, and (c) the complex sequential stress-assisted transformations in Cu–Al–Be single crystals. In this case, the stress-induced transitions are obtained by applying tensile forces to samples with the austenitic axis close to $[001]_{\beta}$.

Concerning the Ni–Ti alloys, an increase of complexity appears when polycrystalline materials are studied, where markedly cycling effects are observed. After cycling, the thick wires of the Ni–Ti alloy display the appearance of S-shaped cycles requiring 600 MPa for a "complete" transformation. The effect can be enhanced up to 1000 MPa using appropriate strain aging at 373 K. See, for instance Ref. [7], where the highly complex processes present during the consecutive transformations were outlined. The study suggests that the MT constitutes an interesting working space in research of guaranteed applications [8] and, also, in fundamental phase transitions [6]. In the following sections, each of the mentioned topics will be presented and shortly analyzed. In some cases, detail on the experimental methods will be summarized, mainly because non-standard equipment was used towards the required precision of the measurements. In every case, more details can be found in the mentioned references where the experiments were originally presented. In general, in the paper we do not consider time effects in the behavior of the studied alloys as, for instance, the martensite stabilization and the beta recovery.

On the Cu-Based Shape Memory Alloys

Cu-based alloys constitute one of the most analyzed groups of SMAs [9–13]. Several reasons justify this interest of the scientific community. On one hand, large mechanical reversibility has been reported for several Cu-based alloys, either ternary or even with higher amount of components. Cost is relatively low if compared with Ni–Ti alloys and additionally melting temperatures are considerably lower than the usual ones reported either for Ni–Ti or for Fe-based alloys. This last point facilitates the preparation of the alloys. On the other hand, problems to be solved in ternary Cu-based alloys are still present, being this the driving force for a large amount of work distributed in several laboratories around the world. Just as a few examples, we can mention the interest in several matters like fatigue behavior [14, 15], different methods of fabrication [16, 17], grain size effects on significant properties like thermal hysteresis [18], analysis of diffusive phenomena like recrystallization [19] and stabilization of martensite [20, 21], and microstructural changes due to severe plastic deformation [22]. The effect of precipitation as a method to modify significant parameters of martensitic transformations has been analyzed by several authors and still deserves attention [23–26]. Searching new potential applications constitutes an additional and permanent task [27]. This short list of topics does not intend to be complete, but suggests that a large amount of research is required for a complete comprehension of these phenomena. As it has been mentioned, three particular cases are chosen to emphasize the complex and particular behavior of the shape memory alloys. The three selected systems, i.e., Cu–Zn–Al, Cu–Al–Ni, and Cu–Al–Be are considered as potential candidates for applications of shape memory effect and pseudoelasticity. Single crystals have been used in the first and third case. Here, the main points to analyze are not affected by the presence of grain boundaries, which are known to alter the mechanical behavior in a strong way.

Intrinsic Thermoelasticity and Pseudoelasticity in Cu–Zn–Al Single Crystals

On the Experimental Details

Standard macroscopic and microscopic techniques have been used: metallographic microscopy, X-rays, TEM, electrical resistance, etc. The measurements have been accomplished using single crystals grown by the Bridgmann technique, with electron concentration around 1.48 and nominal Ms near room temperature. Several heat treatments were used. The standard studies start with sample homogenization (18 min at 1123 K) and then water (TT2: high initial number of dislocations) or air quenched (TT1: very few dislocations) [5]. For instance, some calorimetric samples were cut from a single crystal of a Cu-16.06 at.% Zn-15.97 at.% Al alloy. From the composition, the standard transformation temperature Ms is 230 K. Frequently, a Cu-14.6 at.% Zn-16.7 at.% Al single crystal was used in stress–strain–temperature measurements. The nominal Ms was 288 K. Some resistance measurements were performed in single crystals with the composition Cu-14.6 at.% Zn-16.2 at.% Al. The estimated transformation temperature Ms was 280 K. In stress, strain and temperature analysis, the orientation of the tensile axis was determined with the Laue X-ray method. The variant of martensite which appeared was that with the highest Schmid factor and planar samples, thickness near 1 mm, carefully polished and bone shaped were prepared.

The mesoscopic analysis has been accomplished with the help of especially non-standard adapted devices. In a first step, the study was performed using standard but 'non-classical conduction calorimeters' usually with simultaneous detection of the acoustic emission (A.E.). These systems derived from older systems enable the measurement of the energetic dissipation (heat power).

The non-conventional calorimeter (see Fig. 1) was used for a preliminary evaluation of the alloy behavior in the transformation. The calorimeter (Fig. 1 left) is situated inside a Dewar of 4 L with several disks of isolated materials. Use of liquid nitrogen in the E chamber (in the bottom of the Dewar) permits appropriate spontaneous cooling, for instance, down to 170 K. Displacement to another Dewar with a lower power bulb in the E position permits slow and efficient heating up to 373 K.

Use of old MELCOR plates (Melcor Corp./1040 Spruce St/Trenton NJ 08648/USA) permits reliable non-conventional calorimetric work since the end of the seventies (Fig. 1). One Peltier plate was the basic sensor that allowed to work up to 313 K (in the middle of eighties). An increase of maximal temperature was available using other Peltier/Seebeck elements as, for instance, Dr. Neumann Peltier-Technik GmbH (Gautinger Str. 45/82061 Neuried/Germany) [28, 29].

Figure 2 outlines the device for detailed observation of the MT [30, 31]. The relevant part of the device was a working surface (in Cu) under controlled or programmed temperature. Using a Peltier plate (G) of 40 × 40 mm^2 and varying the DC current, according to the temperature measured by a resistance Pt-100, it is possible to establish an appropriate temperature in the working surface. The working space permits the positioning of two Seebeck plates (C and C′) with sample and reference (D and D′) and, eventually, one piezoelectric disk, detecting the burst of acoustic emission. The signals of C and C′ furnish calorimetric output for the sample associated to the programmed temperature of F plate. The device uses a liquid flow (B, B′) as a temperature reference. The water condensation of the external wet air was avoided using one slow dry air current, i.e., CO_2 (A). The sample surface was observed by an optical microscope (M). The Peltier plates permit efficient control over the temperature of the samples. Using one Pt-100 as a temperature sensor with a resolution of 0.001 Ohm, the device enables to control temperature changes as low as 0.01 K, being this a

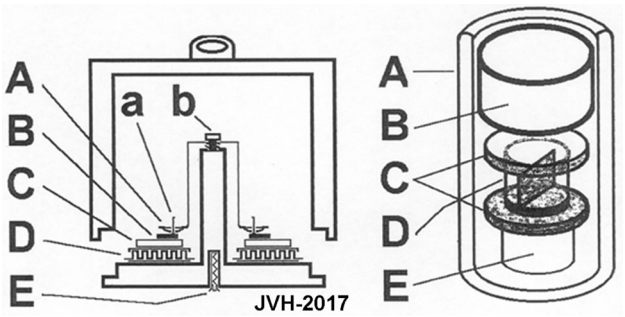

Fig. 1 Left: non-conventional calorimeter in a cooper box. *A* Fixing sample and reference device. *B* Acoustic sensor. *C* Sample. *D* Peltier thermopile (i.e., MELCOR). *E* Temperature sensor (i.e., Pt-100). Right: *A* a four liter Dewar. *B* Isolated disk. *C* Disks of rigid plastic. *D* Calorimetric space. *E* Support permitting a cooling or heating space

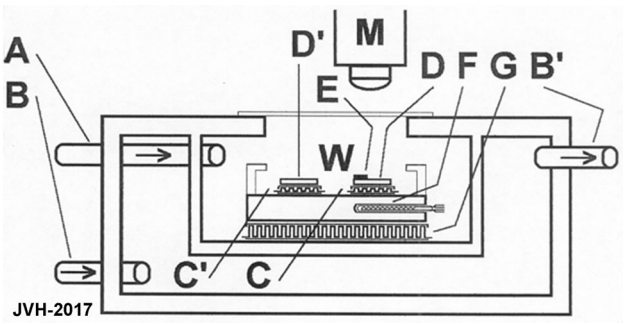

Fig. 2 Programmed working surface and outline of the programmed calorimetric device

significant experimental detail concerning the analysis of the MT.

The Intrinsic Thermoelasticity

The intrinsic thermoelasticity (and pseudoelasticity) could be observed using samples with bone shape, with a rectangular cross section, close to 1 mm^2 and the observation zone was near 2 mm with a thickness close to 0.5 mm. Figures 3 and 4 show the martensite plate for several temperatures on cooling and on heating. Figure 5 shows the different slope $[(\partial x/\partial T)_\sigma]$ of the interface position against the temperature for the TT1 (air-quenched samples) and for TT2 (water quenched).

It was shown that this phenomenon appears due to the interaction of the martensite with the pre-existing dislocations in the parent phase. Due to the different crystallographic structures between the phases, dislocations with Burgers vectors having translation symmetry in the β phase may lose their translation symmetry when absorbed by the martensite. Consequently, every time one of these dislocations is absorbed by the martensite, a stacking fault is dragged by the growing plate. The plate becomes more faulted needing further undercooling to grow. The same phenomenon is observed in stress-induced transformation. Figure 6 outlines the effect, at constant temperature: an increasing stress is applied to force the martensite plate to grow, i.e., a pseudoelastic effect. See Refs. [6, 32, 33] for more details.

Considering the measurements, it was clearly established that, for the widening of a martensite plate, a progressive cooling is strictly necessary and the reverse process needs a "similar" increase of temperature. The observations show "intrinsic" differences with the classical phase equilibrium (i.e., constant temperature or stress), which are mainly associated to the dislocation concentration. The existence of thermoelasticity $[(\partial x/\partial T)_\sigma]$ in the coexistence zone, where x indicates the interface position, establishes the appearance of a related pseudoelasticity $[(\partial x/\partial \sigma)_T]$, being the classical Clausius–Clapeyron equation $[(\partial \sigma/\partial T)_{coex}]$ the link between them.

The Standard Retransformations and the Second β Phase

The work with air-quenched single crystals (with low dislocation concentration) can produce unexpected results. In general, a retransformation recovers the original parent phase in its original orientation: the complex structure of transformed material with several variants of martensite is the only compatible one with the original variant of parent phase. However, one single variant of martensite is compatible with two crystals of the parent β phase which are related by a rotation or/reflection due to the crystal relationship between the involved structures. Using particular experimental conditions and a single plate of martensite, the appearance of a second variant of the β phase was possible. This is an extremely unlikely event [32]. In fact, working with a single martensite plate in the center of an

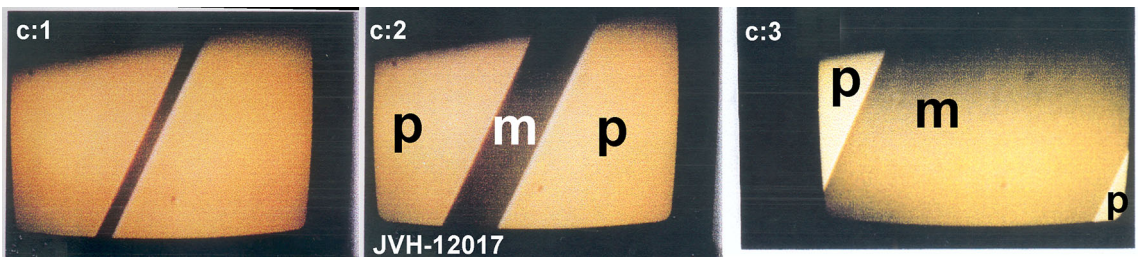

Fig. 3 Thermoelasticity in Cu–Zn–Al, single crystal: interface displacements on cooling (c), respectively (c:1, c:2 and c:3, at 287.15, 285.29 and 285.15 K). In the screen, the sample length was near 1 mm

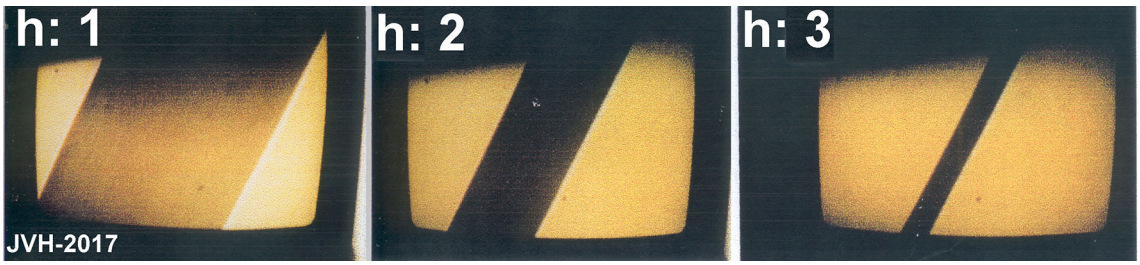

Fig. 4 Thermoelasticity: interface displacements related on heating (h), respectively (h:1, h:2, h:3), at 286.27, 286.35, and 286.49 K) one day after air quench

air-quenched sample (Fig. 7a), a progressive cooling can induce that one side transforms completely into a unique 18R plate without the need of nucleation of additional plates of the same variant. This is only possible if the density of dislocations is extremely low. In this way, this transformed area of the sample is not produced by the coalescence of martensite plates of the same variant (Fig. 7b). Later, heating can produce the nucleation of a new variant ($\beta^{(2)}$) of the parent phase as schematically shown in Fig. 7c. It can be observed in this figure and also in the experimental evidence shown in Fig. 8 that both variants of the β phase differ in shape and orientation. These two variants of the austenite are related by the symmetry operation on the martensite (C_{2h} crystallographic group). The process implies a clear break-down of the shape memory effect [34].

The noticeable output of this experiment is that the behavior of the retransformation into the parent phase in a MT can be strongly modified depending on the concentration of dislocations. This anomalous result in the phase retransformation could be detected using a single-interface transformation which required a precise experimental setup. At low dislocation concentration (i.e., air quenching for Cu–Zn–Al with 1.48 e/a), it is possible for a single martensite variant to retransform into a $\beta^{(2)}$ single crystal differently oriented if compared with the original one ($\beta^{(1)}$). Both β variants are related by a symmetry operation of the 18R martensite. The transformation in a large domain of only one martensite variant using the movement of a single interface was required for this result, which clearly shows a break-down of the known shape memory effect.

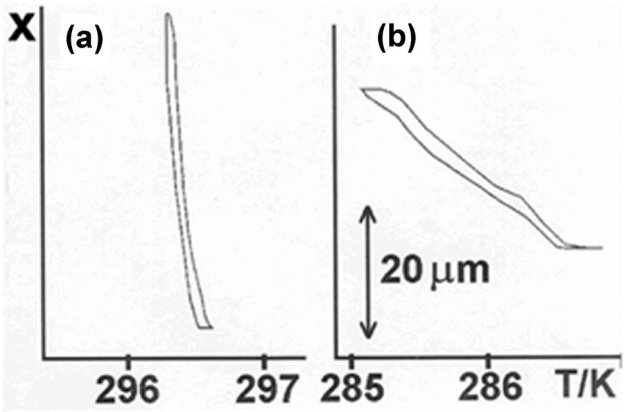

Fig. 5 Outline of the interface position against the sample temperature for air (TT1—**a**) and water quenching (TT2—**b**). The slope was coherent with the dislocation concentration [5, 6]

Two Martensite Phases in Cu–Al–Ni Alloy

Figure 9 shows a calorimetric output (i.e., the thermogram) corresponding to cooling and heating for a polycrystalline sample of Cu–Al–Ni with 6.1 mm of diameter and 0.25 mm in thickness using a device similar to the one outlined in Fig. 1. The samples were thermally treated at 1173 K for 10 min and quenched in iced water. The calorimetric signal visualizes a burst transformation, i.e., from a parent to hexagonal martensite 2H (γ') with an intense acoustic emission. The transformation requires (from Ms to Mf) near 35 K. The retransformation (martensite to parent) shows a separation in two processes. First, indicated by an arrow, one smoothed process as, for instance, 18R (β') to parent and, later, one from hexagonal martensite to parent. The retransformation provides evidence of the appearance of two processes, the first one with thermoelastic character (see the arrow in the m → p thermogram) and later a burst retransformation. The retransformation between As and Af requires near 40 K. The measurements associated to microscopic observations of the sample surface establishes the apparent "coexistence" of β, 2H, and 18R, i.e., parent and two martensites. In fact, it was reported that a shell of parent phase is always present between the martensites [35]. In the absence of applied stresses, the 2H martensite is more stable with respect to the 18R martensite [36]. However, a mixture of the 2H, 18R, and β phases can be observed because of the following two mainly reasons: (a) the large hysteresis of the β-2H transformation (35–40 K) compared to the 18R-β transformation (< 10 K). Thus, on cooling the 18R can

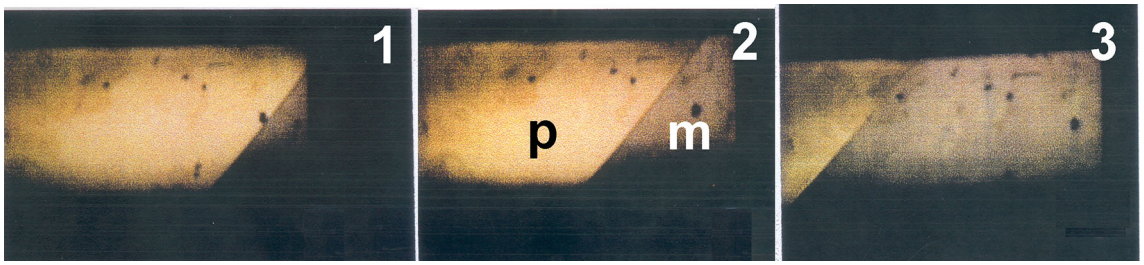

Fig. 6 Pseudoelasticity in single crystal of CuZnAl after air quench. *p* parent phase, *m* martensite. Interface displacements associated with soft hand-operated increasing stress (1 → 2 → 3) at constant temperature (observed length: near 1 mm)

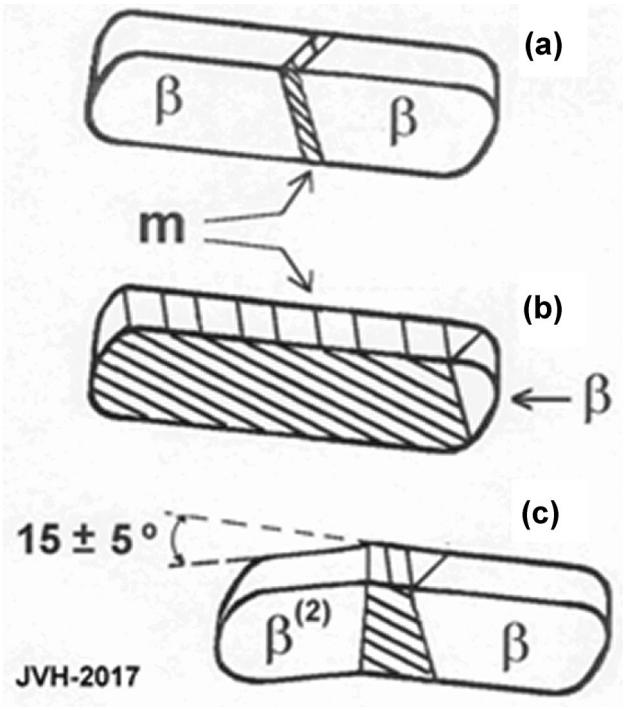

Fig. 7 Appearance of a crystallographic parent phase two ($\beta^{(2)}$). **a** Initial state with a slice of martensite phase between the same variant of parent phase. **b** Complete grow of the martensite in one side of the sample. **c** Appearance of the second variant of parent phase

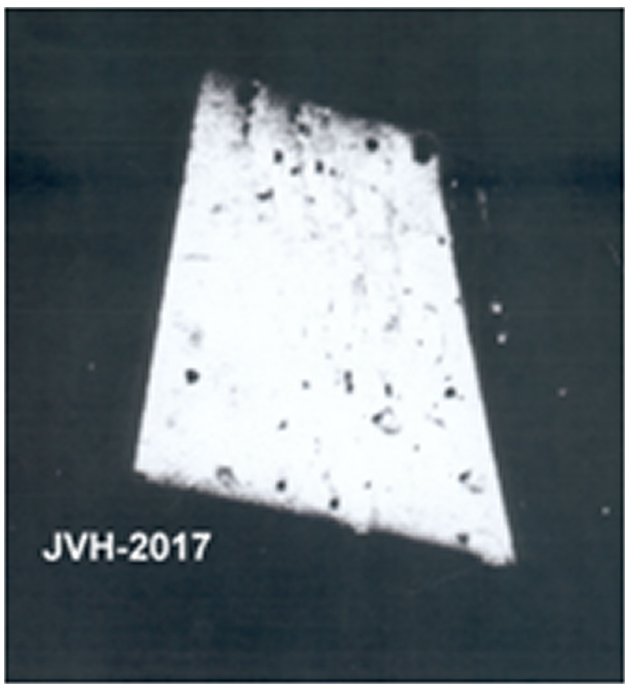

Fig. 8 Martensite phase 18R between two parent phases (i.e., $\beta^{(1)}$ and $\beta^{(2)}$)

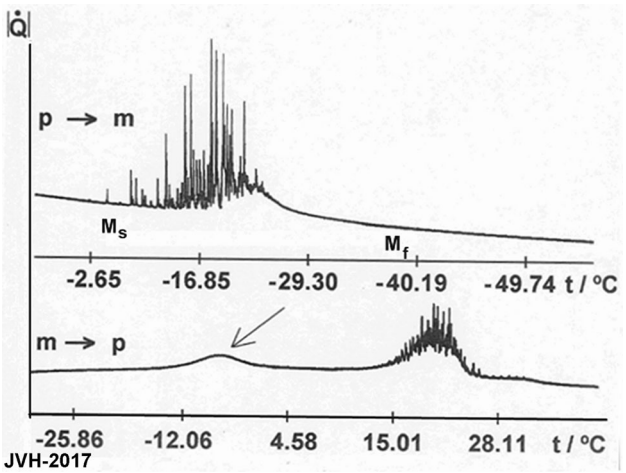

Fig. 9 Cooling (up) and heating (down) of a quenched sample of CuAlNi. The calorimetric signal (in arbitrary units) shows a burst-type transformation. The arrow indicates a "non-burst" or thermoelastic retransformation. The transformation (from Ms to Mf) requires near 35 K

appear before the 2H phase. (b) The presence of dislocations and grain boundaries in the material. It was shown more recently [37] that the interaction of the twinned 2H martensite with dislocations arrays makes the growth of the right relationship between both twinned variants (necessary to form an undistorted habit plane) difficult. This comes from an energetic unbalance due to the different interaction of each twin variant with a dislocation array. Therefore, it becomes more difficult for the 2H martensite to form and to grow. On the other hand, the 18R martensite is almost not affected by the dislocations. Both reasons contribute to inhibit the 2H martensite and to favor the appearance of the 18R martensite.

It is noticed here that in polycrystalline samples of Cu–Al–Ni alloy, in spite of the greater stability of the 2H martensite, progressive cooling induces transformation into a mixture of parent (β), 18R(β′), and twinned hexagonal 2H(γ′) martensites. This is mainly due to two reasons: (a) the large hysteresis of the β-2H transformation (35–40 K) compared to the 18R-β transformation (< 10 K). Thus, on heating the 18R appears before the 2H phase. (b) The dislocations and grain boundaries present in the material, in addition to the dislocations generated by the hexagonal transformation, affect the relative stability between both twinned variants of the 2H phase. In this way, the formation and movement of an undistorted habit plane between the γ′ martensite and the parent phase is more difficult. Then the formation of the 18R structure, having a narrower hysteresis and a rather weaker interaction with the dislocations, is possible.

The Pseudoelastic Behavior of Cu–Al–Be Single Crystals

In polycrystalline alloys, the effect of grain boundaries on the martensitic transformation is quite strong leading to microplasticity phenomena which usually affect pseudoelasticity, since the amount of maximum reversible deformation is reduced [38, 39]. Another significant difference concerns the hysteresis in stress–strain curves, which is strongly affected by the interaction between austenite–martensite interfaces and grain boundaries [39]. The interest on the mechanical behavior of Cu–Al–Be single crystals comes from the presence of sequential martensitic transformations which considerably increases the amount of reversible deformations. From this point of view, this system belongs to a group of alloys with nice and attractive pseudoelastic properties. Examples of sequential stress-induced transformations can be found in several systems. Just as a few examples we can mention Cu–Zn–Al, Cu–Al–Ni, Ni–Fe–Ga, and Ni–Mn–Ga [40–43].

In what follows a short summary of the mechanical behavior of Cu–Al–Be single crystals will be presented [44]. For selected compositions, the β-18R transformation takes place either thermally or by applying a mechanical stress. If the tensile orientation of the β axis is close to $[001]_\beta$, the 6R martensite forms after tensile stressing a 18R single crystal. This enables to get large recoverable deformations, larger than 20%, making this system attractive for potential applications. Moreover, these alloys do not show the same brittleness as the Cu–Al–Ni system, although stabilization of martensite plays a more relevant role in Cu–Al–Be alloys than in the Cu–Al–Ni ones.

It has been reported that critical stresses to transform as well as martensitic transformation temperatures are affected by the state of order of the austenite, the concentration of vacancies, and the stabilization of the martensite [45]. This requires that in order to separate contributions from different parameters, the state of the material must be defined precisely. It has been shown that quenching the stable β structure from high temperature down to 373 K and keeping the material 1 h at this temperature lead to a concentration of vacancies close to the equilibrium one and stable martensitic transformation temperatures [44]. At this state, an interesting behavior is present if a Cu–Al–Be single crystal with orientation of the axis close to $[100]_\beta$ is tensile stressed. An example is shown in Fig. 10, where it can be observed that three transitions can be observed. The first one is the β-18R transition which leads to an 18R single crystal. If these martensitic variant is further stressed, the 18R structure gets distorted into a new phase named 18R′ [44]. This behavior, rather anomalous in Cu-based alloys, can be described as a stress-induced distortion which leads to a small deformation, close to 1%. The

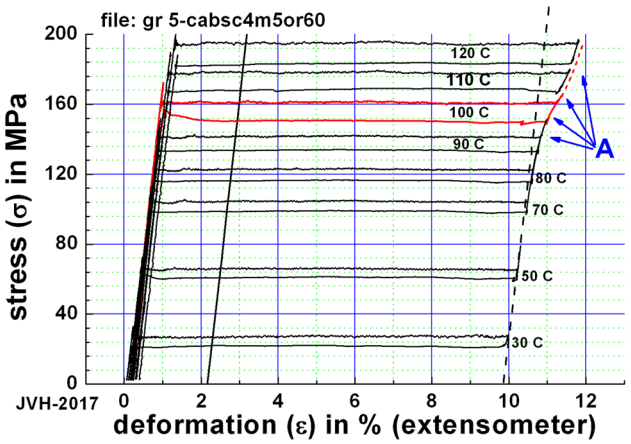

Fig. 10 Stress–strain curves in Cu–Al–Be single crystal at 303 and 393 K. The curves visualize the β-18R transition. The 18R–18R′ structural distortion is observed in loading at 303 K. A partial 18R′–6R transition is shown at 303 K

stress–strain curve does not show a plateau at this transition, showing instead an increase of stress which amounts a value close to 50 MPa (see Fig. 10). A linear relationship between the critical stress to obtain this distortion and the test temperature was measured, in a wide temperature range leading to variations of the critical stress to obtain 18R′ versus temperature equal to 0.42 MPa/K value. It can be easily noticed that the critical stress to distort the 18R structure increases with temperature an amount approximately 5 times smaller than the value reported for the β-18R transformation (1.92 MPa/K). The entropy change associated to this distortion is 50 times smaller than the corresponding one to the β-18R transition, due to the difference in deformation amounts and the reported slopes for both transitions (β-18R and 18R–18R′).

The hysteresis associated to the structural distortion is noticeable small, which makes this transition rather similar to the R phase formation in Ni–Ti alloys. Several interesting features follow from the existence of the 18R–18R′ distortion: (a) the 6R martensite forms from the distorted 18R′ crystal instead from 18R like in the Cu–Zn–Al and Cu–Al–Ni alloys. This has been studied in detail by De Castro Bubani et al. in [46], (b) the hysteresis associated to the β-18R transition increases for temperatures equal or higher than the required one to distort the 18R structure, (c) the critical stresses for the β-18R transformation do not linearly depend on temperature as in most of the martensitic transitions, and finally (d) the deformation associated to the β-18R transition increases with temperature if this one is higher than the required one to start the distortion of 18R [44]. This last point can be noticed in the curves shown in Fig. 11. In this figure, stress–strain curves obtained at different test temperatures are shown. In all cases, the β-18R transformation is complete and it can be

noticed that deformation is larger at higher temperatures. This behavior is clearly anomalous since the deformation associated to a tensile stressed single crystal depends on the orientation of the tensile axis and on composition. This can be explained if we consider that the deformation of the structural distortion increases the corresponding one to the β-18R transition.

As the structural distortion does not have a stress plateau, this effect becomes more visible as the temperature increases in the temperature range where the 18R–18R′ takes place. As it is observed, the presence of the structural distortion obtained by tensile stressing an 18R single crystal modifies the pseudoelastic behavior of Cu–Al–Be single crystals, leading to a mechanical behavior rather different from the usual ones in other Cu-based shape memory alloys. Till the moment only one similar distortion was reported in Cu-based alloys, particularly in Cu–Al–Ni single crystals, taking place in a 2H martensite [47]. This phenomenon was explained by a change in the lattice parameters of the basal plane. Considering that the basal planes of the 18R in Cu–Al–Be alloys and of the 2H martensite in Cu–Al–Ni is the same one, a similar model was used to explain the distortion reported in Cu–Al–Be, which was suitable to rationalize the obtained deformation [44]. A detailed analysis of the 18R′–6R transition has been reported elsewhere and will not be detailed here [46]. However, a few points will be commented in what follows. An interesting property of this transition is the small and negative $d\sigma^{18R-6R}/dT$ slope of this transition (see Table 1). The hysteresis of this transition is considerably larger than the hysteresis found for the β-18R transition. This leads to an additional interesting fact: if the retransformation from 6R martensite takes place at a stress smaller than the corresponding one to the retransformation from 18R, the hysteresis is controlled by the first transition, leading to large hysteresis. This makes this transition an interesting alternative for damping purposes.

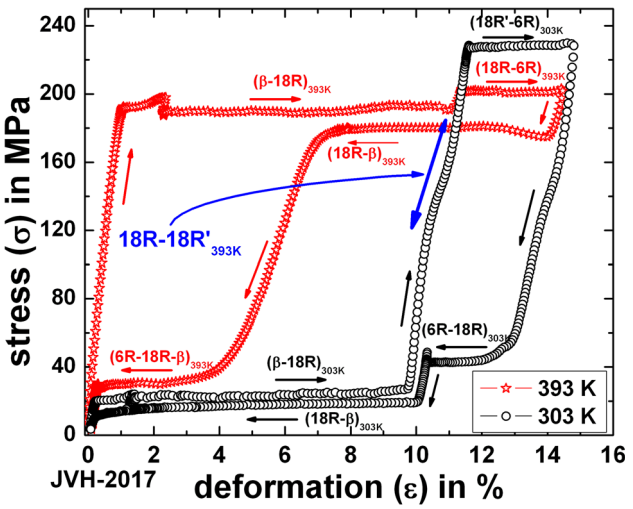

Fig. 11 Series of stress–strain curves showing the β-18R transition at different temperatures (303–393 K). Deformation increases with temperature due to the presence of the 18R–18R′ structural distortion

We notice here that several SMA alloys show the appearance of two consecutive phase transitions. In particular, the Cu–Al–Be single crystal permits a global strain larger than 20% by the stress-induced transition first to 18R and, later to 6R. This behavior is similar to the formation of 6R martensite in Cu–Al–Ni and Cu–Zn–Al single crystals. However, tensile loading Cu–Al–Be single crystals with a progressive stress at T equal or higher than $\sigma\beta^{-18R}$ leads to the appearance of a minor distortion, rather similar to the R transition in Ni–Ti alloys. This 18R–18R′ distortion has a corresponding small deformation (close to 1%) but alters significant parameters of the martensitic transformations of the system.

On the S-Shaped Cycles in Conventional Ni–Ti

Ni–Ti alloys are likely to be one of the most attractive systems concerning applications of shape memory alloys. One of the main reasons for this is their biocompatibility [48–50]. However, non-medical applications are also strongly expected [51]. Several of these applications might use the damping associated to the martensitic transformation. Particularly large amounts of energy originated in natural events could be dissipated using the pseudoelastic effect of Ni–Ti alloys, and this is undoubtedly an attractive possibility [52–54]. A practical and also relevant point is that Ni–Ti alloys are provided by industrial manufacturers accomplishing reproducible properties. Any new application will surely profit from the availability of Ni–Ti alloys in different shapes. An extended review on the shape memory properties of these alloys is far from the scope of the present study and in fact we will focus on a specific mechanical behavior and its relationship with linear defects. However, a few comments might be useful for the reader before introducing a detailed result.

Table 1 Slopes of the linear relationships between critical transformation stresses and temperature, determined for each martensitic transition in a Cu–Al–Be single crystal of composition Cu-11.4 wt% Al-0.53 wt% Be (Cu-22.63 at.% Al, 3.15 at.% Be)

Martensitic transition	$d\sigma/dT$ to start the transition in MPa/K
β-18R	0.42
18R–18R′	1.92
18R′–6R	− 0.29

The first aspect to be mentioned is the effect of composition on Ni–Ti shape memory properties. A nice discussion was presented several years ago by Saburi [55]. One of the main points addressed by this author is that Ni-rich alloys (> 50.5 at.%) show nicer pseudoelastic properties, while binary Ni–Ti alloys with Ni content smaller than 50.5 at.% seem to show better shape memory behavior and less favorable pseudoelastic properties [56]. However, it has been reported that both shape memory and pseudoelasticity effects can be improved by hardening the matrix of any of these compositions [57]. In fact if the matrix is sufficiently hard, nice superelastic behavior is found for Ni contents lower than 50.5 at.%, of course at test temperatures higher than Af. An example of this has been reported in [58] where the author shows reproducible and large pseudoelastic behavior for a Ni content equal to 50.2 at.% if test temperature is high enough. One of the main reasons to consider larger Ni contents as more favorable for the presence of pseudoelasticity is the introduction of coherent Ti_3Ni_4 precipitates. A large amount of work has been devoted to increase the comprehension of the effect of these precipitates on the martensitic transformation [59, 60]. There is no doubt that the presence of these precipitates is positive for the improvement of shape memory properties and pseudoelasticity. Different reasons have been considered for this, being two relevant ones: (a) internal stresses introduced by these precipitates which favor the transformation to R phase previous to the transformation to B19′ martensite and (b) the increase in matrix hardness [60]. Once it was understood that a harder matrix plays a significant role in favoring shape memory and pseudoelastic properties, a large amount of work was devoted to obtain a larger hardness using other methods like the introduction of dislocations and the controlled change of grain size. In fact excellent mechanical behavior associated to pseudoelastic transformation has been obtained for Ni–Ti alloys with Ni content equal or larger than 50.7 at.%Ni and nanograins [61]. Straight annealing at temperatures close to 773 K after cold work leads to a density and distribution of dislocations extremely favorable to obtain pseudoelastic behavior [62]. Finally, it should be considered that different thermal treatments usually performed and reported lead to the simultaneous action of several factors, like precipitation, particular distribution of dislocations, and nanograin size.

Another interesting matter to consider is the effect of adding ternary elements or even quaternary ones to the Ni–Ti binary system. However, if compared with systems we have considered above, it should be taken into consideration that addition of ternary elements in Cu-based alloys has been unavoidable to get usable martensitic transformation temperatures. Just as an example, shape memory properties are far better in Cu–Zn–Al and Cu–Al–Ni alloys if compared with binary Cu–Zn and Cu–Al alloys. On one hand, the addition of ternary components enables the selection of martensitic transformation temperatures in a temperature range which enhances potential applications [63]. On the other hand, the addition of ternary components has specific positive effects which are not only the variation of Ms. An example of this can found in Cu–Al–Ni alloys where the addition of Ni has a slighter effect of Ms if compared with Al, but avoids diffusion in the alloy preventing in this way precipitation of equilibrium phases [63]. A different situation arises if Ni–Ti alloys are considered, where critical transformation temperatures for a large amount of different purposes can be easily obtained controlling the amount of Ni in the binary system. In fact a detailed analysis of the effect of composition on Ms has been reported by Frenzel et al. [64], where Ms varies from 340 K down to 210 K in the composition range from approximately 50.0 at.% Ni up to 51.2 at.% Ni. In spite of this, the effect of adding ternary elements has been largely analyzed leading to interesting results [55]. Just to mention a few examples reported by Saburi in this reference, Ms decreases if Ti atoms are substituted by V, Cr, Mn, and Al. The addition of Co and Fe atoms replacing Ni atoms also leads to a decrease of Ms. Ms might also increase, which has been verified by the addition of Au and Pd. The addition of Zr or Hf also increases Ms [64]. One of the interesting consequences of adding a ternary element is the different effect of the addition on each of martensitic transformations taking place, i.e., formation of martensite B19′ and the R phase transition. A particular and attractive result has been reported for Ti–Ni–Cu alloys, since adding Cu not only decreases Ms corresponding to the monoclinic B19′ martensite, but also shows a decrease in thermal hysteresis and the transition from the B2 austenite into an orthorhombic B19 structure if Cu content is larger than approximately 7.5 at.%, which has a hysteresis smaller than the corresponding one to form B19′ from B2 [65, 66]. A smaller hysteresis reported in Ti–Ni–Cu alloys than the present one in binary alloys leads to consider these alloys suitable for shape memory actuators. A nice and detailed analysis of the effect of ternary elements on Ms and other properties is presented in [64].

In what follows, a specific result will be analyzed in the frame of the present study where the interaction between linear defects and the pseudoelastic behavior is visible. The Ni–Ti alloy was provided by SAES Getters (Milan, Italy) via a subsidiary company Memry Corp. (Bethel CT, USA) and was previously provided by Special Metals Corp. (New Hartford, New York, USA). The surface of the samples was finished with a light (gray) oxide surface (for the 2.46-mm-diameter A wires) or with black oxide (for the 0.5-mm-diameter B wires). The nominal As temperatures for the A and B wires were similar at 248/247 and 243 K,

respectively. The furnisher indicated that the nominal wire composition was 50.9 at.% Ni for wires A and B.

In this case, the experiment consists in performing about one hundred of stress–strain cycles at 0.01 Hz, in wires of Ni–Ti of 2.46 mm of diameter with a maximal deformation of eight per cent (Fig. 13). After the cycles, a permanent deformation (SMA "creep") of 2% is observed. In addition, the morphology of the stress–strain curve changes after cycling. While a nice plateau is observed for cycle 1 (transformation stress close to 600 MPa), transformation stresses decrease during cycling, being the stress reduction dependent on the amount of transformation. Thus, the transformation curve shows an S-shaped cycle. The reduction of the transformation stress increases for larger amounts of transformation. Conversely, the variations of retransformation stresses do not significantly change.

Keeping damper applications in mind, it can be emphasized that although the hysteresis cycles are markedly reduced during the first cycles, the shape of the cycles (and the total hysteresis area) becomes more and more stable after a few tenth of cycles. Then a nearly asymptotic behavior is achieved. In this final state, the hysteresis and the energy dissipation capacity are still important for many applications.

It should be also remarked that ambient temperature changes will also affect the transformation. The Clausius–Clapeyron coefficient establishes a displacement of the base-line position of 6.3 MP/K. Temperatures as 253 K (i.e., − 20 °C) (see the horizontal line near the 250 MPa in Figs. 2, 3, 4, 5, 6, 7, 8, 9, 10, 11, 12) modifies the hysteretic cycle but the working cycles permit a lesser, but still relevant, damping effect. Working at 253 K (− 20 °C), the hysteresis cycle was approximately reduced to the upper "half" and appropriately modified. The S-shaped can be improved using strain aging at 373 K. The effect of strain and temperature (373 K) increases the maximal stress up to 1000 MPa [8].

The diameter of the wires has also an important effect on the shape of the stress strain curves. For example, a wire of 0.5 mm of diameter shows a flat behavior. The evolution after 100 cycles with a maximal strain of 8% produces a different behavior as compared to the just mentioned wire of 2.46 mm of diameter. Figure 13 includes cycles 1 and 100 in similar conditions as in Fig. 12. The SMA creep is similar but the hysteresis cycles remain flat although the transformations stress decreases practically to half of the initial value. The change of shape induces completely different behavior if variations of ambient temperature are considered. At low room temperature (as 253 K), the thin wire remains practically in martensite. For thinner wire at 273 K, the material cannot retransform and, for cycles at

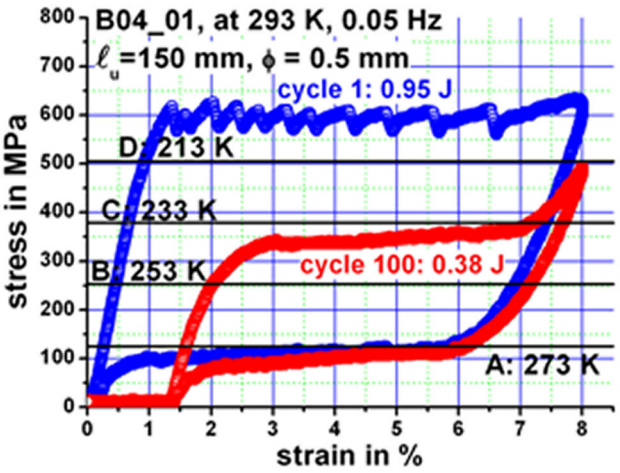

Fig. 13 NiTi thin wire with a diameter of 0.5 mm. *A*, *B*, …, *D*, base-line position, respectively, for 0 °C, − 20 °C, …,− 60 °C

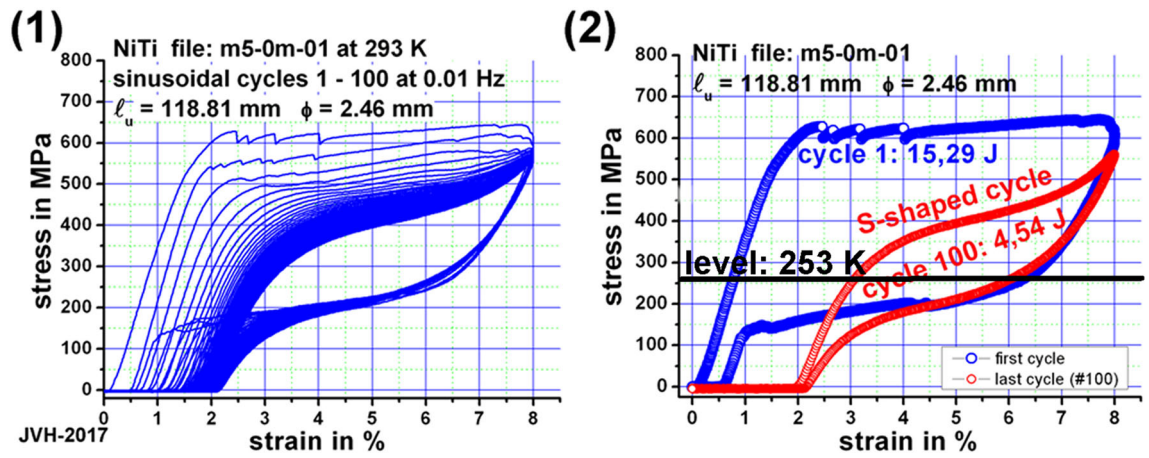

Fig. 12 Ni–Ti stress–strain cycles with a strain up to 8%. **1**: The first cycle shows a nearly constant transformation stress and, after cycling, appears a SMA creep near 2% and a change of the shape to S-shaped cycles. **2**: Differences between the cycle 1 and the cycle 100. The level at 253 K relates the position of the base line for an external temperature of − 20 °C

temperatures as low as − 40 °C the wire transforms and, later, remains always in martensite.

Microstructural changes after cycling were analyzed by transmission electron microscopy by Condó et al. [67]. These authors reported a high density of dislocations and concluded that most likely the reduction of critical transformation stresses are related to the energy spent in creating those dislocations, which in turn have a favorable interaction with the martensite in the subsequent cycles. In addition, it is expected that a low ratio between grain size and specimen diameter would need a higher degree of plastic deformation for the shape change accommodation. Hence, dislocations with many Burgers vectors would be created particularly at higher strains. These dislocations would compete with the previous ones, now producing a gradually increase of the transformations stresses as the strain increases. The mechanisms of this latter effect would be the same as those mentioned in the previous paragraph for Cu-based alloys. Both are expected to take place from B2 to the B19′ twinned martensite in Ni–Ti.

The main outputs are mentioned in what follows. During pseudoelastic cycling, thick wires (2.46 mm of diameter) show a markedly decrease of intermediates transformation stresses, depending on the amount of strain. Permanent deformation (martensite "creep") of about 2% remains in the material. After a few tenth of cycles, a stable behavior is achieved with an S-shaped stress–strain cycles. On the other hand, a thinner wire (0.5 mm diameter) shows a different behavior; the stresses to transform decrease on cycling but the curves remain rather flat. A creation of a high density of favorable dislocations explains the strong reduction in the transformation stresses. In thicker wires, a higher degree of plastic deformation is expected for the grain accommodation according to the shape change imposed by the martensitic transformation. These dislocations, competing with the previous ones, would produce a gradually increase of the transformation stresses as the strain increases. The mechanisms would be the same as those mentioned in the previous paragraph 2.1.2 and 2.2 for Cu-based alloys. Both are expected to take place from the B2 parent phase to the B19′ twinned martensite in Ni–Ti. The S-shape provides a wanted behavior for some applications (e.g., dampers) when working in cool winters in comparison with thin wires. The latter easily remain in martensite (when working below $\approx$ 254 K) reducing or impeding a convenient performance.

Conclusions

The study of the MT suggests a complex behavior in comparison with classical equilibrium phase transition, i.e., performed at constant intensive thermodynamic variables. The thermoelasticity/pseudoelasticity establishes that the transformation requires progressive cooling or increased stress. Dislocations play the main role in order to explain the origin of intrinsic thermoelasticity. At low dislocation concentration, and using a single-interface transformation, a second β phase crystal can be formed during retransformation from martensite, breaking in this way the shape memory effect.

Interaction between dislocations and martensitic transitions where two martensites are formed (β′ and γ′) can explain the change in metastable phase diagrams where the relative phase stability is modified enhancing the formation of β′.

The mechanical behavior of β single crystals of Cu–Al–Be alloys shows a particular behavior if compared with other Cu-based alloys. The stress-induced 18R phase gets structurally distorted while being further loaded, this new phase being the one which transforms into 6R martensite.

Strong differences can be found in the mechanical evolution after pseudoelastic cycling if Ni–Ti wires with different diameters are used. After cycling, the thick wires show an "S-shaped" hysteretic cycle. The transformation requires progressive stress up to 600 MPa. The S-shaped cycles are of practical interest for working under the external winter temperatures. The samples can transform at reduced working temperature in comparison with thinner wires that, at similar temperatures, remain in martensite. A high density of dislocations was reported to explain this strong evolution in the mechanical behavior.

Acknowledgements Technical supports from the Materials Laboratory of the Atomic Center of Bariloche, 8400 Argentina, and in Department of Structural Mechanics in Pavia University (Italy), the facilities in stayed cables of ELSA, Ispra, Italy, and the cable studies of IFSTTAR, Bouguenais, France, are gratefully acknowledged. Prof. Jan Van Humbeeck, we have a great pleasure contributing with this paper in occasion of your retirement. We thank you very much for your wide and fruitful contributions on many fields of metallurgy and particularly on martensitic transformations. We shall keep great remembers of our joint research, discussions, and collaborations over more than 30 years of exciting research activities. Your laboratory at the KUL was a pleasant place where we found your kind friendship and your knowledge to enrich our research. You have also traveled across the world visiting many countries. We remember your stay at the UIB (Balearic Islands) and the CAB (Bariloche, Argentina) where we accomplished interesting joint work on Shape Memory Alloys, particularly in Copper-based and Ni–Ti alloys. Many conferences like ESOMAT and ICOMAT gave us the opportunity to attend your lectures and to have interesting discussions enlightening our ideas. Dear colleague, we wish you a happy retirement and full and long life accompanied with relatives and friends.

References

1. Ehrenfest P (1933) Phase changes in the ordinary and extended sense classified according to the corresponding singularities of the thermodynamic potential (Verhandelingen der Koninklijke

Akademie van Wetenschappen. Amsterdam). Proc Acad Sci Amsterdam 36:153–157
2. Landau LD (1937) Zur Theorie der phasenumwandlungen II. Phys Z Sowjetunion 11:26–35
3. Lovey FC (1982) Relationship between surface martensite, thin foil and bulk martensite. Journal de Physique, Colloque 4 43:C4-585–C4-590
4. Otsuka K, Wayman CM (1998) Introduction in shape memory materials, 1st edn. Cambridge University Press, Cambridge, pp 1–26
5. Lovey FC, Amengual A, Torra V, Ahlers M (1990) On the origin of the intrinsic thermoelasticity associated with a single-interface transformation in Cu–Zn–Al shape memory alloys. Philos Mag A 61:159–165
6. Lovey FC, Torra V (1999) Shape memory in Cu-based alloys: phenomenological behavior at the mesoscale level and interaction of martensitic transformation with structural defects in Cu–Zn–Al. Prog Mater Sci 44:189–289
7. Torra V, Auguet C, Isalgue A, Carreras G, Lovey FC (2013) Metastable effects on martensitic transformation in SMA. Part IX. Static aging for morphing by temperature and stress. J Therm Anal Cal 112:777–780
8. Torra V, Isalgue A, Sade M, Lovey FC (2015) Shape memory alloys as an effective tool to damp oscillations: study of the fundamental parameters required to guarantee technological applications. J Therm Anal Cal 119(3):1475–1533
9. Ahlers M (1986) Martensite and equilibrium phases in Cu–Zn and Cu–Zn–Al alloys. Prog Mater Sci 30(3):135–186
10. Wollants P, Roos JR, Delaey L (1993) Thermally- and stress-induced thermoelastic martensitic transformations in the reference frame of equilibrium thermodynamics. Prog Mater Sci 37(3):227–288
11. Otsuka K, Ren X (1999) Martensitic transformations in nonferrous shape memory alloys. Mater Sci Eng A 273–275:89–105
12. La Roca PM, Isola LM, Sobrero CE, Vermaut P, Malarría J (2015) Grain size effect on the thermal-induced martensitic transformation in polycrystalline Cu-based shape memory alloys. Mater Today 2:S743–S746
13. Tuncer N, Qiao L, Radovitzky R, Schuh CA (2015) Thermally induced martensitic transformations in Cu-based shape memory alloy microwires. J Mater Sci 50:7473–7487
14. Shrestha KC, Araki Y,Kusama T, Omori T, Kainuma R (2016) Functional fatigue of polycrystalline Cu–Al–Mn superelastic alloy bars under cyclic tension. J Mater Civ Eng 28. Article number 04015194
15. Yan H, Marcoux Y, Chen Y (2017) Cyclic mechanical properties of copper-based shape memory alloys: the effect of strain accommodation at grain boundaries. Int J Fatigue 105:1–6
16. Li DY, Zhang SL, Liao WB, Geng GH, Zhang Y (2016) Superelasticity of Cu–Ni–Al shape-memory fibers prepared by melt extraction technique. Int J Miner Metall Mater 23:928–933
17. Donoso GR, Walczak M, Moore ER, Ramos-Grez JA (2017) Towards direct metal laser fabrication of Cu-based shape memory alloys. Rapid Prototyp J 23:329–336
18. La Roca P, Isola L, Vermaut Ph, Malarría J (2017) Relationship between grain size and thermal hysteresis of martensitic transformations in Cu-based shape memory alloys. Scr Mater 135:5–9
19. Lima EPR, De Lima PC, Nava M (2016) Determination of recrystallization kinetics and activation energy of grain growth process of Cu–14Al–4Ni shape memory alloy. Mater Res Soc Symp Proc 1765:127–132
20. Saposhnikov Golyandin, Kustov S, Cesari E (2008) Defect-assisted diffusion and kinetic stabilization in Cu–Al–Be β_1' martensite. Mater Sci Eng A 481–482:532–537
21. Sade M, Pelegrina JL, Yawny A, Lovey FC (2015) Diffusive phenomena and pseudoelasticity in Cu–Al–Be single crystals. J Alloy Compd 622:309–317
22. Figueroa CG, García-Castillo FN, Jacobo VH, Cortés-Pérez J, Schouwenaars R (2017) Microstructural and superficial modification in a Cu–Al–Be shape memory alloy due to superficial severe plastic deformation under sliding wear conditions. In: IOP Conference Series: Materials Science and Engineering, 194. Article Number 012011
23. Zárubová N, Gemperle A, Novák V (1997) Initial stages of γ_2 precipitation in an aged Cu–Al–Ni shape memory alloy. Mater Sci Eng 222:166–174
24. Araujo VEA, Gastien R, Zelaya E, Beiroa JI, Corro I, Sade M, Lovey FC (2015) Effects on the martensitic transformations and the microstructure of CuAlNi single crystals after ageing at 473 K. J Alloys Compd 41:155–161
25. Cuniberti A, Montecinos S, Lovey FC (2009) Effect of γ^2-phase precipitates on the martensitic transformation of a β-CuAlBe shape memory alloy. Intermetallics 17:435–440
26. Bubani FDC, Lovey FC, Sade M (2017) A short review on the interaction of precipitates and martensitic transitions in CuZnAl shape memory alloys. Funct Mater Lett 10(1):1740006-1–1740006-8
27. Huang H, Wang W, Liu J, Xie J (2016) Progress on the applications of Cu-based shape memory alloys. Mater China 35:919–926
28. Tachoire H, Macqueron JL, Torra V (1986) Signal treatments in microcalorimetry-applications in kinetics and Thermodynamics. Thermochim Acta 105:333–367
29. Torra V, Tachoire H (1998) Conduction calorimeters- heat transmission systems with uncertainties. J Thermal Anal Cal 52(3):663–681
30. Isalgue A, Torra V (1993) High-resolution equipment for martensitic transformation in shape memory alloys: local studies in stress-strain-temperature. Meas Sci Technol 4:456–461
31. Amengual A, Torra V (1989) An experimental set-up for thermal analysis and DSC—its application to the hysteresis cycles in shape memory alloys. J Phys E 22(7):433–437
32. Lovey FC, Isalgue A, Torra V (1992) Hysteresis loops in stress-induced β-18R martensite transformation in Cu–Zn–Al. Acta Metall Mater 40(12):3389–3394
33. Amengual A, Lovey FC, Torra V (1990) The hysteretic behavior of a single interface martensitic-transformation in Cu–Zn–Al shape memory alloys. Scr Metall Mater 24(12):2241–2246
34. Lovey FC, Amengual A, Torra V (1991) Experimental and crystallographic evidence for the growth of two equivalents ß-variants from one single martensite plate in a Cu–Zn–Al single crystal. Philos Mag A 64(4):787–796
35. Van Humbeeck J, Van Hulle D, Delaey L, Ortin J, Segui C, Torra V (1987) A two-stage martensite transformation in a Cu-13.99 mass% Al-3.5 mass% Ni alloy. Trans JIM 28(5):382–391
36. Gastien R, Corbellani CE, Sade M, Lovey F (2004) Thermodynamical aspects of martensitic transformations in CuAlNi single crystals. Scr Mater 50(8):1103–1107
37. Gastien R, Sade M, Lovey FC (2008) Interaction between martensitic structure and defects in $\beta - \beta' + \gamma'$ cycling in CuAlNi single crystal. Model for the inhibition of γ' martensite. Acta Mater 56:1570–1576
38. Montecinos S, Cuniberti A (2008) Thermomechanical behavior of a CuAlBe shape memory alloy. J Alloys Compd 457(1–2):332–336
39. Sade M, de Castro Bubani F, Lovey F, Torra V (2014) Effect of grain size on stress induced martensitic transformations in a Cu–Al–Be polycrystalline shape-memory alloy: pseudoelastic cycling effects and microstructural modifications. Mater Sci Eng A 609:300–309

40. Barceló G, Ahlers M, Rapacioli R (1979) Stress induced phase transformation in martensitic single crystal of CuZnAl alloys. Mater Res Adv Tech 70(11):732–738
41. Otsuka K, Wayman CM (1998) Mechanism of shape memory effect and superelasticity. In: Otsuka K, Wayman CM (eds) Shape-memory materials. Cambridge University Press, Cambridge, pp 27–48
42. Hamilton RF, Sehitoglu H, Efstathiou C, Maier HJ (2007) Inter-martensitic transitions in Ni–Fe–Ga single crystals. Acta Mater 55:4867–4876
43. Hamilton RF, Sehitoglu H, Aslantas K, Efstathiou C, Maier HJ (2008) Inter-martensite strain evolution in NiMnGa single crystals. Acta Mater 56(10):2231–2236
44. Sade M, Yawny A, Lovey FC, Torra V (2011) Pseudoelasticity of Cu–Al–Be single crystals: unexpected mechanical behavior. Mat Sci Eng A 528:7871–7877
45. González CH, De Araújo CJ, Quadros NF, Guénin G, Morin M (2004) Study of martensitic stabilisation under stress in Cu–Al–Be shape memory alloy single crystal. Mater Sci Eng A 378:253–256
46. Bubani FDC, Sade M, Torra V, Lovey FC, Yawny A (2013) Stress induced martensitic transformations and phases stability in Cu–Al–Be shape-memory single crystals. Mat Sci Eng A583:129–139
47. Arneodo Larochette P, Condó AM, Ahlers M (2005) Stability and stabilization of 2H martensite in Cu–Zn–Al single crystals. Philos Mag 85:2491–2525
48. Miyazaki S (1998) Medical and dental applications of shape memory alloys. In: Otsuka K, Wayman C (eds) Shape memory materials. Cambridge University Press, Cambridge, pp 267–281
49. Duerig T, Pelton A, Stockel D (1999) An overview of nitinol medical applications. Mater Sci Eng A 273–275:149–160
50. Song C, Frank TG, Cuschieri A (2003) Application of high-pushing-force NiTi for minimal access surgery. J Phys IV 112:1133–1136
51. Van Humbeeck J (1999) Non-medical applications of shape memory alloys. Mater Sci Eng A 273–275:134–148
52. Dolce M, Cardone D (2006) Theoretical and experimental studies for the application of shape memory alloys in civil engineering. J Eng Mater Technol Trans ASME 128:302–311
53. Song G, Ma N, Li HN (2006) Applications of shape memory alloys in civil structures. Eng Struct 28:1266–1274
54. Cardone D, Dolce M (2009) SMA-based tension control block for metallic tendons. Int J Mech Sci 51:159–165
55. Saburi T (1998) Ti–Ni shape memory alloys. In: Otsuka K, Wayman CM (eds) Shape memory materials. Cambridge University Press, Cambridge, pp 49–96
56. Saburi T, Tatsumi T, Nenno S (1982) Effects of heat treatment on mechanical behavior of Ti–Ni alloys. J Phys 43:C4-261–C4-266
57. Miyazaki S, Ohmi Y, OtsukaK Suzuki Y (1982) Characteristics of deformation and transformation pseudoelasticity in Ti–Ni alloys. J Phys 43:C4-255–C4-260
58. Puertas GM (2006) Caracterización de materiales con memoria de forma base NiTi para diseño de acoples/Characterization of Ni-Ti Materials with shape memory for desing of coupling devices. Proyecto Integrador Ingeniería Mecánica, Universidad Nacional de Cuyo, Instituto Balseiro
59. Zhou N, Shen C, Wagner MF, Eggeler G, Mills MJ, Wang Y (2010) Effect of Ni4Ti3 precipitation on martensitic transformation in Ti–Ni. Acta Mater 58:6685–6694
60. Wang X, Kustov S, Li K, Schryvers D, Verlinden B, Van Humbeeck J (2015) Effect of nanoprecipitates on the transformation behavior and functional properties of a Ti-50.8 at.% Ni alloy with micron-sized grains. Acta Mater 82:224–233
61. Yawny A, Sade M, Eggeler G (2005) Pseudoelastic cycling of ultra-fine-grained NiTi shape-memory wires. Int J Mater Res (Zeitschrift für Metallkunde) 96:608–618
62. Vojtěch D, Voděrová M, Kubásek J, Novák P, Šedá P, Michalcová A, Fojt J, Hanuš J, Mestek O (2011) Effects of short-time heat treatment and subsequent chemical surface treatment on the mechanical properties, low-cycle fatigue behavior and corrosion resistance of a Ni-Ti (50.9 at.% Ni) biomedical alloy wire used for the manufacture of stents. Mater Sci Eng A 528:1864–1876
63. Tadaki T (1998) Cu-based shape memory alloys. In: Otsuka K, Wayman CM (eds) Shape memory materials. Cambridge University Press, Cambridge, pp 97–116
64. Frenzel J, Wieczorek A, Opahle I, Maaβ B, Drautz R, Eggeler G (2015) On the effect of alloy composition on martensite start temperatures and latent heats in Ni–Ti-based shape memory alloys. Acta Mater 90:213–231
65. Nam TH, Saburi T, Shimizu K (1990) Cu-content dependence of shape memory characteristics in Ti–Ni–Cu alloys. Mater Trans JIM 31(11):959–967
66. Grossmann C, Frenzel J, Sampath V, Eggeler G (2009) Elementary transformation and deformation processes and the cyclic stability of NiTi and NiTiCu shape memory spring actuators. Metall Mater Trans A 40:2530–2544
67. Condó AM, Lovey FC, Olbricht J, Somsen Ch, Yawny A (2008) Microstructural aspects related to pseudoelastic cycling in ultra fine grained Ni–Ti. Mater Sci Eng A 481–482:138–141